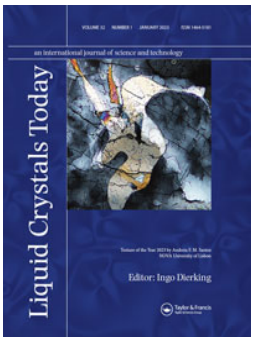

Liquid Crystals Today

ISSN: (Print) (Online) Journal homepage: www.tandfonline.com/journals/tlcy20

Development of ionic liquid crystals based on pyridinium and picolinium cations

Andreia F. M. Santos

To cite this article: Andreia F. M. Santos (2023) Development of ionic liquid crystals based on pyridinium and picolinium cations, Liquid Crystals Today, 32:1, 4-11, DOI: 10.1080/1358314X.2023.2221615

To link to this article: https://doi.org/10.1080/1358314X.2023.2221615

© 2023 The Author(s). Published by Informa UK Limited, trading as Taylor & Francis Group.

Published online: 04 Jul 2023.

Submit your article to this journal

Article views: 564

View related articles

View Crossmark data

Full Terms & Conditions of access and use can be found at
https://www.tandfonline.com/action/journalInformation?journalCode=tlcy20

LIQUID CRYSTALS TODAY
2023, VOL. 32, NO. 1, 4–11
https://doi.org/10.1080/1358314X.2023.2221615

ARTICLE

OPEN ACCESS

Development of ionic liquid crystals based on pyridinium and picolinium cations

Andreia F. M. Santos

LAQV-REQUIMTE, Department of Chemistry, NOVA School of Science and Technology, NOVA University of Lisbon, Caparica, Portugal

ABSTRACT

The search for novel materials and technologies with improved performance increased in the last decades. In particular, ionic liquid crystals (ILCs), a modern class of advanced materials that benefits from the synergistic properties of ionic liquids and liquid crystals, are playing an important role in different areas of knowledge, attracting the interest of the academia and industry, driven by their peculiar tailoring ability. Herein, it comprises a brief synopsis of several pyridinium and picolinium ILCs previously prepared to understand how their mesomorphism and conductivity profiles are affected by small structural changes in terms of the methyl group position and alkyl chain length, providing important insights into future design of functional materials by a simple anionic exchange. Moreover, microwave-assisted reactions were emphasised as a simple and greener synthetic method to prepare ionic liquid crystals through alkylation, which can also be applied to other organic salts.

KEYWORDS

Ionic liquid crystals; pyridinium & picolinium salts; Differential Scanning Calorimetry (DSC); Polarised Optical Microscopy (POM); X-Ray Powder Diffraction (XRD); Dielectric Spectroscopy (DS)

Introduction

Ionic liquids (ILs), i.e., organic salts with low melting point, have proven to be useful in a wide range of applications (Figure 1), from tailor-made solvents [1–4] (the first generation of ionic liquids) to advanced materials [5–8] (second generation) and pharmaceuticals [9–12] (third generation), due to the wise pairing of their cations and anions, allowing to modulate the final properties of the compound [13–16]. This fine tuning, extremely relevant in several fields, is addressed by the huge diversity of ions that can be incorporated in ionic liquids. Indeed, it is possible to couple organic, inorganic, chiral or achiral moieties, as well as entirely or partially ionised acids and bases, charged bridging ligands, metallated coordination polymers, organic polymeric metal ions and amino acids [16]. Most of the structures reported are based on substituted organic cations (e.g., imidazolium, pyridinium, pyrrolidinium, ammonium and phosphonium) and inorganic anions (e.g., halides, perchlorates, tetrafluoroborates and hexafluorophosphates) [16,17]. However, multiple ILs containing organic anions were developed with triflates, bistriflimides, benzoates, alkylsulfates, alkylcarbonates, carboxylates, among other anions [16,17]. In addition, ionic liquids are known for their low volatility, although some of them can be distilled under specific conditions [18], high chemical and thermal stability, being also excellent conductors with a large electrochemical window [19,20]. Liquid crystals (LCs), on the other hand, are anisotropic compounds with intermediate characteristics of both crystalline solids and isotropic liquids [21–25]. These fluids exhibit long-range orientational order, along with birefringence, fluidity and the ability to self-assemble, as well as other specific properties that highlight the relevance of these materials in modern science and industry [26–30]. Additionally, mesophases emerging upon temperature or concentration/solvent variations are designated as thermotropic or lyotropic liquid crystals, respectively. Different molecular structures, associated with the chemical properties and molecular geometry of LCs, lead to distinct liquid crystalline phases, ranging from nematic (N) to smectic (S), columnar (Col) and cubic (Cub) phases [31]. Among these phases, nematic is the one presenting higher fluidity, while smectic phases are recognised for displaying lamellar molecular organisation. In particular, the molecular arrangement of smectic layers is responsible for the formation of different mesophases, such as S_A, S_B, S_C, S_F and S_G phases [32]. Furthermore, when a certain material has liquid crystalline properties and is simultaneously ionic, it can be classified as ionic liquid crystal (ILC) [32–35].

Nowadays, with global warming and other environmental concerns, there is a huge demand for sustainable chemical processes, opening doors to the use of alternative solvents (e.g., ionic liquids, deep eutectic solvents and supercritical fluids), solventless systems, microwave-assisted reactions, mechanochemistry and flow chemistry

CONTACT Andreia F. M. Santos afm.santos@campus.fct.unl.pt

© 2023 The Author(s). Published by Informa UK Limited, trading as Taylor & Francis Group.
This is an Open Access article distributed under the terms of the Creative Commons Attribution License (http://creativecommons.org/licenses/by/4.0/), which permits unrestricted use, distribution, and reproduction in any medium, provided the original work is properly cited. The terms on which this article has been published allow the posting of the Accepted Manuscript in a repository by the author(s) or with their consent.

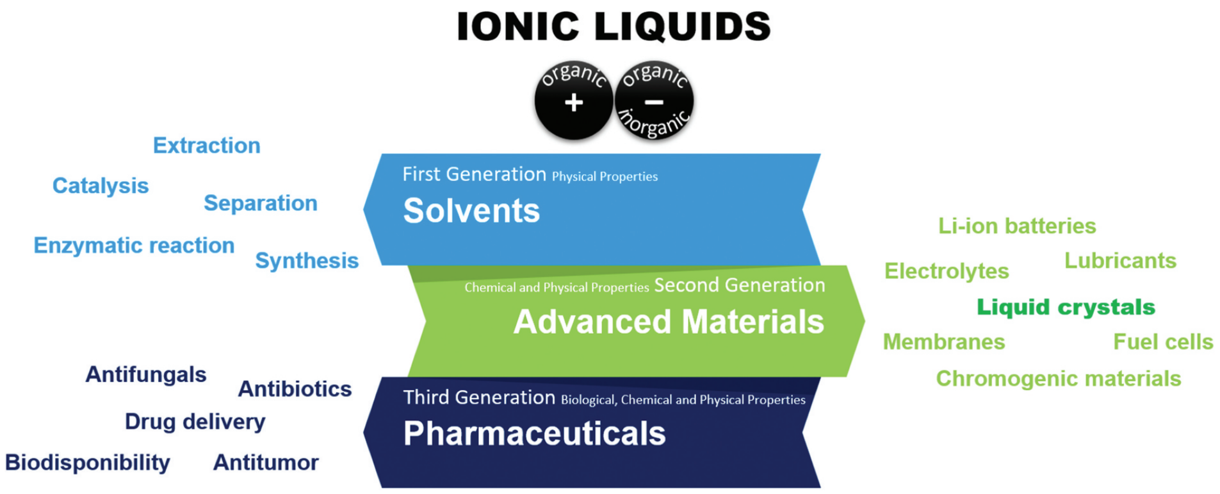

Figure 1. Three generations of ionic liquids and examples of their respective applications.

[36–40]. The search for greener methodologies is also important in the preparation of different ionic systems (organic salts, ionic liquids, ionic liquid crystals, among others). Typically, there are two synthetic steps involved in the preparation of ionic liquids: alkylation reaction to obtain the desired cation using the selected haloalkanes, followed by anionic exchange reaction, which can be through metathesis or acid–base processes [17,41]. Therefore, ILs based on halides can be considered templates for synthesising task-specific materials. However, several studies have been focused on these starting organic salts to fully understand their properties before functionalise them [42–46]. In this context, most of the ionic liquid crystals reported are based on an aromatic ring coupled with a long alkyl group and, thus, originating salts with rod-like structures. This molecular shape is known for promoting the appearance of lamellar phases. On the other hand, discotic conformations are addressed to the emergence of columnar phases, being less common in ionic liquids with liquid crystalline character. In fact, K. Binnemans and co-workers [47] provided an intensive overview of the mesogenic structures associated with thermomesomorphism, emphasising also the intensive exploration of this field towards the design of novel functional materials. The latter includes electronic applications in sustainable energy storage and conversion devices, such as battery electrolytes, supercapacitors, fuel cells and dye-sensitised solar cells [48,49], pointing out ionic liquid crystals as alternatives to conventional materials [50,51]. There are several reasons to advantageously use ILCs in such applications: the already mentioned ability to order and self-assemble in a diversity of arrangements, endorsing multidimensional ion conductive pathways [52,53], high cohesion energy to the electrode surface [54], multiple types of cation–anion interactions, varying from electrostatic and Van der Waals interactions to conventional and non-conventional hydrogen bonds [55–57], as well as high electrochemical stability and enlarged voltage window [58,59].

In this context, several pyridinium and picolinium (methylpyridinium) ionic liquid crystals have been synthesised through sustainable methods and further characterised by thermal, microscopic and spectroscopic techniques. Herein, an overview of how the methyl group position [60] and the alkyl chain length [61] impact their mesomorphism and conductive behaviour is provided, guiding also the design of new functional materials.

Sustainable synthesis of ionic liquid crystals

Concerning the preparation of novel ionic liquids with mesogenic properties, there is a crucial aspect to be considered: the design of ILCs with calamitic shapes is highly impacted by the alkyl chain length. Smaller sizes impair the formation of liquid crystalline phases, turning the material crystalline, while higher chains promote increased mobility that can mitigate the long-distance orientational order, a critical feature to have in mind when it is intended to support the molecular self-assembly. Indeed, sizes between C_6 and C_{18} are reported as being suitable to form liquid crystals [34,62–64]. Therefore, 1-dodecylpyridinium bromide ($[C_{12}Pyr][Br]$) and 1-dodecyl-*n*-methylpyridinium bromide ($[C_{12}\text{-}n\text{-}Pic][Br]$, $n = 2$, 3 or 4) were synthesised to understand the influence of the methyl group position in their mesomorphic behaviour. Furthermore, to expand the studies regarding modifications at the molecular level, two other potential ILCs were prepared, changing the size of the aliphatic tail, to compare with $[C_{12}\text{-}2\text{-}Pic][Br]$:

1-hexyl-2-methylpyridinium bromide ([C_6-2-Pic][Br]) and 1-hexadecyl-2-methylpyridinium bromide ([C_{16}-2-Pic][Br]).

As previously mentioned, the search for sustainable alternatives to conventional methods has increased in the last few decades. Under this perspective, two strategies were used to synthesise the pyridinium and picolinium organic salts highlighted in the present manuscript: conventional heating and microwave irradiation. In both cases, the desired compounds were successfully prepared. However, microwave-assisted reactions revealed to be more efficient and greener processes, as no solvent is needed and the alkylations can be completed with higher yields (87–96% *vs.* 34%) and purity levels in less time (35–50 min *vs.* 48 h). Additionally, since the materials were prepared in neat conditions, the purification process was also simplified. It was found that, compared to similar cations, the syntheses of the 2-picolinium organic salts were more challenging to obtain good yields, probably due to their methyl group at *ortho-* position, which confers stereochemical hindrance, impairing the functionalisation with long alkyl chains.

Mesomorphic behaviour

Effect of the methyl group position

In order to assess the liquid crystalline behaviour of [C_{12}Pyr][Br], [C_{12}-2-Pic][Br], [C_{12}-3-Pic][Br] and [C_{12}-4-Pic][Br], all materials were characterised by Differential Scanning Calorimetry (DSC), Polarised Optical Microscopy (POM) and X-Ray Powder Diffraction (XRD) to evaluate, respectively, their phase transformations, textures and structural properties [60]. Figure 2 comprises the microphotographs acquired within the mesophase of each organic salt.

Thermotropic transitions with different liquid crystalline windows were found for all samples, confirmed by the presence of sharp calorimetric transformations (DSC), birefringent domains and fluidity (POM), as well as specific scattering patterns with signals at small angles (XRD). Moreover, the intensive thermal treatment performed by DSC, between –90°C and 200°C, carried out at 2, 5 and 10°C min^{-1}, allowed to infer about their resistance upon successive cooling and heating runs. In this context, all materials exhibited high thermal stability with no signs of degradation. Comparing the second and the fourth scans, [C_{12}Pyr][Br] ($T_{Cr\rightarrow LC} = 59°C$; $\Delta T_{LC} = 65°C$) stood out from the other homologous salts due to its wide mesomorphic window on heating and cooling, as well as after overcycling. It also showed a homeotropic alignment, responsible for the light extinction in some preparation's regions when the sample is between two glass plates, which hindered the observation under crossed polarisers. On the other hand, for [C_{12}-2-Pic][Br] ($T_{Cr\rightarrow LC} = 77°C$; $\Delta T_{LC} = 47°C$), the stiffness provided by the methyl group at *ortho-* position promoted the appearance of an ordered LC phase, suggested by the low enthalpy involved in the conversion from crystal to liquid crystal and later confirmed by XRD with the simultaneous rise of peaks at small and large angles. This higher rigidity also reflects a superior tendency to crystallise, being the only one that turned monotropic on cooling. Regarding [C_{12}-3-Pic][Br] ($T_{Cr\rightarrow LC} = 61°C$; $\Delta T_{LC} = 12°C$) and [C_{12}-4-Pic][Br] ($T_{Cr\rightarrow LC} = 48°C$; $\Delta T_{LC} = 22°C$), both presented reduced thermomesomorphic range in the second heating run, exhibiting focal conics and clearing points below

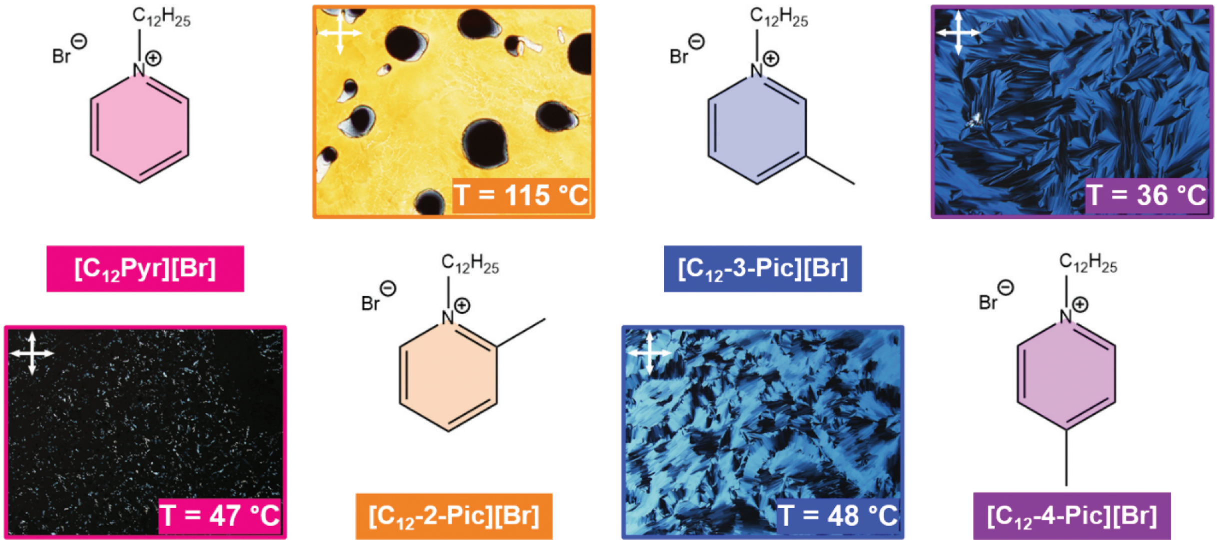

Figure 2. Chemical structures and optical microphotographs associated with the liquid crystalline phases of the ILCs highlighted in the study of the methyl group position: S_A for all materials, excepting for [C_{12}-2-Pic][Br] that displays a S_1 phase.

100°C. Under thermal cycling, these two ILCs lost their mesomorphism, which was recovered after a definite period of time. Finally, the X-Ray Powder Diffraction analysis allowed a deep insight into the molecular ordering, revealing bilayer disordered smectic A (S_A) phases for all materials, except for [C_{12}-2-Pic][Br], whose diffractogram is coherent with an ordered smectic (S_1) phase. Furthermore, it was found that the layers are interdigitated, since their layer spacing is inferior to an integer multiple of the respective cation size.

Effect of the alkyl chain length

Aiming to correlate the lengthening of the alkyl group with the presence of liquid crystalline phases, a shorter ([C_6-2-Pic][Br]) and a longer ([C_{16}-2-Pic][Br]) salts were prepared. They were thermally, optically and structurally characterised, and their behaviour was compared with [C_{12}-2-Pic][Br], being depicted in Figure 3 the textures observed between crossed polarisers. Moreover, the weight loss profile of the three organic salts was also evaluated [61].

Although C_6 has been reported to be suitable for imprinting mesomorphic behaviour [64], no thermotropic transitions were observed for [C_6-2-Pic][Br] ($T_m =$ 88°C), being the diffraction signature coherent with a material in a semi-crystalline state. Moreover, it easily avoids crystallisation on cooling, vitrifying below −25°C, whereas amorphisation of C_{12} and C_{16} was not achieved under the tested conditions. Furthermore, even though thermogravimetric assays revealed a major loss starting at 190 – 200°C for the three 2-picolinium salts, the shortest ionic liquid exhibited signs of degradation upon thermal cycling, contrary to the longer ILCs that are more thermoresistant. On the other side, [C_{16}-2-Pic][Br] ($T_{Cr \rightarrow LC} = 101$°C; $\Delta T_{LC} = 19$°C) exhibited polymorphism, similar to C_{12}, converting to a disordered lamellar phase (S_A) with interdigitated bilayers, whose endotherm is detected even after successive calorimetric runs.

In this section, all samples were monitored on heating and cooling through XRD, disclosing a smectic A phase for [C_{12}-2-Pic][Br]. Hence, this material presents two different LC phases: S_1 on heating and S_A under cooling. The latter is the one conserved upon overcycling.

Table 1 summarises the physical state and the thermotropic behaviour of each organic salt, including the temperature values for the main transitions, the mesomorphic window and the respective structural characterisation. It is worth noting that some materials exhibited a shift towards higher temperatures between the conversion to liquid crystal in the first and second heating runs.

Conductivity behaviour

Effect of the alkyl chain length

Envisaging future applications in the electronic field, [C_6-2-Pic][Br], [C_{12}-2-Pic][Br] and [C_{16}-2-Pic][Br] were characterised by Dielectric Spectroscopy (DS) between −90°C and 160°C. In this context, their conductivity and impedance were measured as a function of frequency and temperature, allowing to investigate the impact of increasing the aliphatic tail on these properties [61].

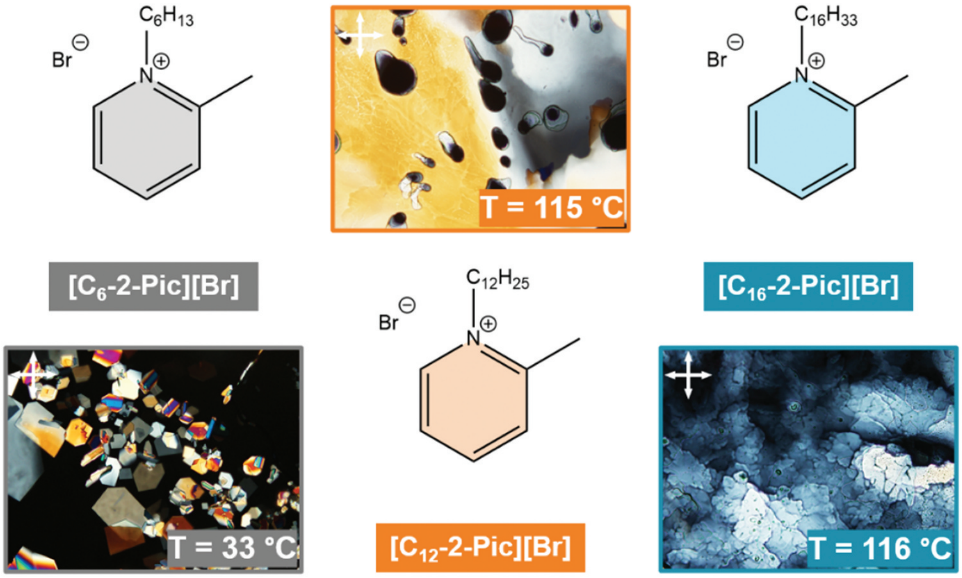

Figure 3. Chemical structures and optical microphotographs addressed to the representative phases of the ILs involved in the study of the alkyl chain length: semi-crystal for [C_6-2-Pic][Br], S_1 for [C_{12}-2-Pic][Br] and S_A for [C_{16}-2-Pic][Br].

Table 1. Physical state and thermomesomorphic behaviour of each organic salt during heating.

		[C_{12}Pyr][Br]	[C_{12}-2-Pic][Br]	[C_{12}-3-Pic][Br]	[C_{12}-4-Pic][Br]	[C_6-2-Pic][Br]	[C_{16}-2-Pic][Br]
Physical state		Cr	Cr	Cr + LC	Cr + LC	sCr	Cr
$T_{Cr\rightarrow LC}$ (°C)	1st	48.31	81.67	27.04	*n.d.*[a]	-	99.34
	2nd	59.17	76.84	6.83	47.68	-	101.04
ΔT_{LC} (°C)		65	47	12	22	-	19
$T_{Cr/LC\rightarrow I}$ (°C)		124.19	123.46	73.28	69.25	87.82	120.51
Mesophase		S_A	S_1[b]	S_A	S_A	-	S_A

With the exception of ΔT_{LC} (liquid crystalline range), all values correspond to the peak temperature of the phase transitions. In order to mitigate the impact of the water content in the material's thermal response, both ΔT_{LC} and $T_{Cr/LC\rightarrow I}$ were determined in the second run. Cr - crystal phase; LC - general liquid crystal phase; sCr - semi-crystal phase; I - isotropic phase; S_A - smectic A phase; S_1 - smectic phase with ordered layers.

[a] The ill-defined endotherms found in the first heating run impaired the accurate analysis of this scan.

[b] SA emerges on cooling.

Moreover, the absence of a clear response associated with dipolar relaxation processes led to the conclusion that all ILs are mainly dissociated in their respective 2-methylpyridinium cations and bromide anions.

For all organic salts, the conductivity spectra resemble those exhibited by a variety of semi-conducting materials [65], where it is possible to distinguish, in different isotherms, two regions: one dependent on the frequency and the other one independent, similar to a plateau. The first is due to a short-distance semi-diffusive charge transport mechanism, while the latter is originated by a long-distance diffusive charge migration regime, named as direct current conductivity (σ_{dc}). Furthermore, a closer inspection of the [C_6-2-Pic][Br] conductivity spectra, collected below 0°C, revealed a decrease at low frequencies owing to ions that accumulate at the sample/electrode interface without discharging, creating an additional capacitance and, thus, reducing the charge transfer. This phenomenon is called electrode polarisation and, for some applications, represents a disadvantage. For the longer salts, this bending off was absent almost up to isotropisation.

It was also possible to establish a general correlation between conductivity and phase transformations of the three salts, since the rise of the direct current plateau is associated with the materials' physical state. In fact, it was found that DS is even more sensitive to changes in the physical state than DSC. Moreover, the temperature dependence of σ_{dc} allowed to construct an activation map, providing a fingerprint of the materials' charge transport. When C_{12} and C_{16} are crystalline and liquid crystalline, a linear behaviour (Arrhenian) with different slopes was observed, characteristic of a thermal activated charge migration mechanism. On the other hand, supercooled C_6 exhibited a curved profile, following a VFTH law, signature of a glass transition assisted mechanism [66], changing to an Arrhenius-type dependence upon cold crystallisation. From the linear branches, the activation energy (E_a) for charge migration was calculated, showing, for [C_{16}-2-Pic][Br], superior values when charges migrate within the crystalline phases in comparison to the LC. Differently, for C_{12}, E_a remains almost invariant along the different phases, acting as additional evidence of the smectic 1 ordering. These results indicate a strong dependence of conductivity relative to the materials' physical state. Thus, care must be taken while comparing their properties at a definite temperature.

From the conductivity measurements, it was possible to estimate the cationic and anionic diffusion coefficients, relevant to the performance of electronic devices [67], contributing to a wise design of novel functional materials [68]. Since bromide is common to the three salts, and the main responsible for charge transport, the substantial differences registered in the conductive and diffusional behaviours of the three salts allowed to infer that the cation also plays a role.

Finally, to further explore C_{12} and C_{16} responses at room temperature, their frequency-dependent impedance spectra (Bode plot) were modelled by an equivalent non-ideal RC electrical circuit, giving rise to a 'depressed' semi-circle in the alternative Nyquist plot representation. The extracted resistance (R) and capacitance (C) values showed that charge propagation in the crystalline state was mainly conditioned by R, being ~40 times higher for the lengthiest salt, while C keeps the same order.

These results, along with conductivity traces in the activation map, allowed to distinguish the charge migration pathways of crystalline and liquid crystalline phases. This was rationalised in terms of i) a charge hopping motion through defects in the crystalline lattice, occurring longitudinally to the chain length, and ii) charge migration in between layers in the mesophase, being almost independent of the alkyl size. A general illustration of these mechanisms is depicted in Figure 4, including a scheme for the respective energy barriers.

Conclusions

In the framework of the 'Liquid Crystal Art Image of the Year 2022' award by The International Liquid Crystal Society, the thermomesomorphic behaviour of six ionic liquids containing pyridinium and picolinium

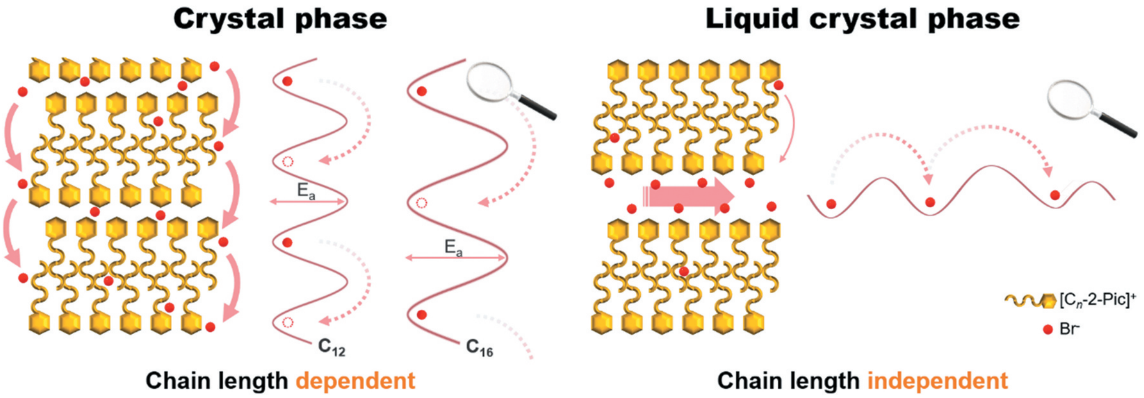

Figure 4. A schematic illustration of the charge transport mechanisms in the crystal and liquid crystal phases of $[C_{12}\text{-2-Pic}][Br]$ and $[C_{16}\text{-2-Pic}][Br]$. For the mesophase, the thickness of the arrows denotes the dominant pathway. The energy barriers are also depicted, in which both activation energy and time between jumps are higher for C_{16}.

(methylpyridinium) cations is outlined. It was possible to identify bilayer interdigitated smectic phases in five of the investigated salts, leading to classify them as ionic liquid crystals. Moreover, a detailed study of chemical modifications was performed in what concerns the effect of the methyl group position (unsubstituted, *ortho*-, *meta*- and *para*-) and alkyl chain length (C_6, C_{12} and C_{16}). In the latter, further Dielectric Spectroscopy measurements were carried out and modelled, allowing to understand how the size of the aliphatic group impacts the conductivity, impedance and ionic diffusion. The information provided by this ongoing project will guide the wise preparation of task-specific ionic liquid crystals through sustainable methods.

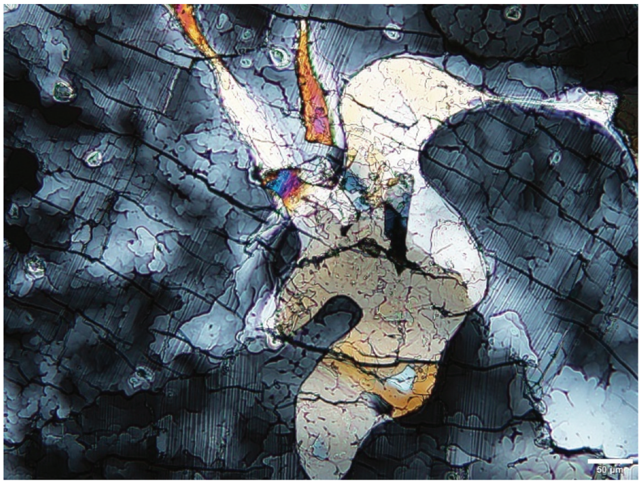

'Flying Colibri', the Liquid Crystal Art Image of the Year 2022 by Andreia F. M. Santos, NOVA University of Lisbon, Portugal.

Acknowledgements

Firstly, I would like to express my gratitude to my PhD supervisors (Prof. Luis C. Branco, Prof. Madalena Dionísio and Prof. Maria H. Godinho) for their guidance, inspiration and support throughout my doctoral project. I am also grateful for the fruitful discussions and help provided by Prof. João L. Figueirinhas and Prof. C. J. Dias.

Disclosure statement

No potential conflict of interest was reported by the author.

Funding

This work was financially supported by the Associate Laboratory for Green Chemistry LAQV [UID/QUI/50006/2019] and the project number [PTDC/EAM-AMB/2023/2021] financed by National Funds through FCT-MCTES and POR Lisboa 2020. The author also acknowledges FCT-MCTES for the PhD Grant [SFRH/BD/132551/2017].

ORCID

Andreia F. M. Santos http://orcid.org/0000-0002-9395-3112

References

[1] Rogers RD, Seddon KR. Ionic liquids - solvents of the future? Science. 2003;302:792–793.
[2] Zalewska K, Branco LC. Organocatalysis with chiral ionic liquids. Mini Rev Org Chem. 2014;11:141–153.
[3] Ventura SPM, E Silva FA, Quental MV, et al. Ionic-liquid-mediated extraction and separation processes for bioactive compounds: past, present, and future trends. Chem Rev. 2017;117:6984–7052.
[4] Hejazifar M, Lanaridi O, Bica-Schröder K. Ionic liquid based microemulsions: a review. J Mol Liq. 2020;303:112264.
[5] Marr PC, Marr AC. Ionic liquid gel materials: applications in green and sustainable chemistry. Green Chem. 2015;18:105–128.

[6] Tang S-F, Mudring A-V. Highly luminescent ionic liquids based on complex lanthanide saccharinates. Inorg Chem. 2019;58(17):11569–11578.

[7] Tiago GAO, Matias IAS, Ribeiro APC, et al. Application of ionic liquids in electrochemistry—recent advances. Molecules. 2020;25:5812.

[8] Donato MT, Colaço R, Branco LC, et al. A review on alternative lubricants: ionic liquids as additives and deep eutectic solvents. J Mol Liq. 2021;333:116004.

[9] Hough WL, Smiglak M, Rodríguez H, et al. The third evolution of ionic liquids: active pharmaceutical ingredients. New J Chem. 2007;31(8):1429–1436.

[10] Pedro SN, Freire CSR, Silvestre AJD, et al. The role of ionic liquids in the pharmaceutical field: an overview of relevant applications. Int J Mol Sci. 2020;21(21):8298.

[11] Nikfarjam N, Ghomi M, Agarwal T, et al. Antimicrobial ionic liquid-based materials for biomedical applications. Adv Funct Mater. 2021;31(42):2104148.

[12] Liu C, Chen B, Shi W, et al. Ionic liquids for enhanced drug delivery: recent progress and prevailing challenges. Mol Pharm. 2022;19(4):1033–1046.

[13] Welton T. Room-temperature ionic liquids. Solvents for synthesis and catalysis. Chem Rev. 1999;99(8):2071–2084.

[14] Plechkova NV, Seddon KR. Applications of ionic liquids in the chemical industry. Chem Soc Rev. 2008;37(1):123–150.

[15] Lei Z, Chen B, Koo Y-M, et al. Introduction: ionic liquids. Chem Rev. 2017;117(10):6633–6635.

[16] Shamshina JL, Zavgorodnya O, Rogers RD. Ionic liquids. Encyclopedia of analytical science. 3rd ed. Elsevier Inc; 2019.

[17] Singh SK, Savoy AW. Ionic liquids synthesis and applications: an overview. J Mol Liq. 2020;297:112038.

[18] Earle MJ, Esperança JMSS, Gilea MA, et al. The distillation and volatility of ionic liquids. Nature. 2006;439(7078):831–834.

[19] Hallett JP, Welton T. Room-temperature ionic liquids. Solvents for synthesis and catalysis. 2. Chem Rev. 2011;111:3508–3576.

[20] Kianfar E, Mafi S. Ionic liquids: properties, application, and synthesis. Fine Chem Eng. 2020;2:22–31.

[21] de Gennes P-G, Prost J. The physics of liquid crystals (international series of monographs on physics). Oxford Science Publications; 1995.

[22] Mohanty S. Liquid crystals- the “fourth” phase of matter. Resonance. 2003;8:52–70.

[23] Dunmur D, Luckhurst G. 38. Liquid crystals. Springer Handb Electron Photonic Mater. 2007. p. 917–952.

[24] Collings PJ, Hird M. Introduction to liquid crystals: chemistry and physics. Introd Liq Cryst Chem Phys. 2017.

[25] Andrienko D. Introduction to liquid crystals. J Mol Liq. 2018;267:520–541.

[26] Oliveira LBA, de Oliveira RP, Oliveira C, et al. Cosmetic potential of a lyotropic liquid crystal emulsion containing resveratrol. Cosmetics. 2017;4(4):54

[27] Inoue M. Review of various measurement methodologies of migration ion influence on LCD image quality and new measurement proposal beyond LCD materials. J Soc Inf Disp. 2020;28(1):92–110.

[28] Kato T, Gupta M, Yamaguchi D, et al. Supramolecular association and nanostructure formation of liquid crystals and polymers for new functional materials. Bull Chem Soc Jpn. 2021;94(1):357–376.

[29] Uchida J, Soberats B, Gupta M, et al. Advanced functional liquid crystals. Adv Mater. 2022;34(23):2109063.

[30] Zhang P, de Haan LT, Debije MG, et al. Liquid crystal-based structural color actuators. Light: Sci Appl. 2022;11(1):248.

[31] Singh S. Phase transitions in liquid crystals. Phys Rep. 2000;324(2–4):107–269.

[32] Salikolimi K, Sudhakar AA, Ishida Y. Functional ionic liquid crystals. Langmuir. 2020;36(40):11702–11731.

[33] Knight GA, Shaw BD. 121. Long-chain alkylpyridines and their derivatives. New examples of liquid crystals. J Chem Soc. 1938;682–683.

[34] Alvarez Fernandez A, Kouwer PHJ. Key developments in ionic liquid crystals. Int J Mol Sci. 2016;17(5):731.

[35] Kapernaum N, Lange A, Ebert M, et al. Current topics in ionic liquid crystals. Chempluschem. 2022;87(1):e202100397.

[36] Gawande MB, Bonifácio VDB, Luque R, et al. Solvent-free and catalysts-free chemistry: a benign pathway to sustainability. ChemSusChem. 2014;7(1):24–44.

[37] Clarke CJ, Tu W-C, Levers O, et al. Green and sustainable solvents in chemical processes. Chem Rev. 2018;118(2):747–800.

[38] Zuin VG, Eilks I, Elschami M, et al. Education in green chemistry and in sustainable chemistry: perspectives towards sustainability. Green Chem. 2021;23(4):1594–1608.

[39] Chen T-Y, Hsiao YW, Baker-Fales M, et al. Microflow chemistry and its electrification for sustainable chemical manufacturing. Chem Sci. 2022;13(36):10644–10685.

[40] Hessel V, Tran NN, Asrami MR, et al. Sustainability of green solvents - review and perspective. Green Chem. 2022;24:410–437.

[41] McIntosh AJS, Griffith J, Gräsvik J. Methods of synthesis and purification of ionic liquids. Appl Purif Recover Ion Liq. Elsevier B.V.; 2016. p. 59–99.

[42] Kumar S, Pal SK. Ionic discotic liquid crystals: synthesis and characterization of pyridinium bromides containing a triphenylene core. Tetrahedron Lett. 2005;46(23):4127–4130.

[43] Ferreira AJ, Cruz C, Godinho MH, et al. Shear-induced lamellar ionic liquid-crystal foam. Liq Cryst. 2010;37(4):377–382.

[44] Luo J, Zhang L, Lu J, et al. Polymerised ionic liquid crystals bearing imidazolium and bipyridinium groups. Liq Cryst. 2017;44(8):1293–1305.

[45] Nestor ST, Heinrich B, Sykora RA, et al. Methimazolium-based ionic liquid crystals: emergence of mesomorphic properties via a sulfur motif. Tetrahedron. 2017;73(36):5456–5460.

[46] Li Z, Ma C, He M, et al. Synthesis and characterization of ionic liquids [C_{12}mim]Cl, [C_{14}mim]Cl and [C_{16}mim]Cl: experimental and molecular dynamics simulations. Liq Cryst. 2022;49(11):1436–1447.

[47] Goossens K, Lava K, Bielawski CW, et al. Ionic liquid crystals: versatile materials. Chem Rev. 2016;116(8):14643–4807.

[48] Devaki SJ, Sasi R. Ionic liquids/ionic liquid crystals for safe and sustainable energy storage systems. Progress

and developments in ionic liquids. London: IntechOpen; 2017.
[49] Quevillon MJ, Whitmer JK. Charge transport and phase behavior of imidazolium-based ionic liquid crystals from fully atomistic simulations. Materials. 2018; 11(1):64.
[50] Sasi R, Sarojam S, Devaki SJ. High performing biobased ionic liquid crystal electrolytes for supercapacitors. ACS Sustain Chem Eng. 2016;4(6):3535–3543.
[51] Gao N, He Y, Tao X, et al. Crystal-confined freestanding ionic liquids for reconfigurable and repairable electronics. Nat Commun. 2019;10(1):1–11.
[52] Yuan F, Chi S, Dong S, et al. Ionic liquid crystal with fast ion-conductive tunnels for potential application in solvent-free Li-ion batteries. Electrochim Acta. 2019;294: 249–259.
[53] Ruan Q, Yao M, Yuan D, et al. Ionic liquid crystal electrolytes: fundamental, applications and prospects. Nano Energy. 2023;106:108087.
[54] Liu H, Liu Y, Li J. Ionic liquids in surface electrochemistry. Phys Chem Chem Phys. 2010;12(8):1685–1697.
[55] Dong K, Zhang S, Wang Q. A new class of ion-ion interaction: z-bond. Sci China Chem. 2015;58(3):495–500.
[56] Dong K, Zhang S, Wang J. Understanding the hydrogen bonds in ionic liquids and their roles in properties and reactions. Chem Commun. 2016;52(41):6744–6764.
[57] Wang Y, He H, Wang C, et al. Insights into ionic liquids: from Z-Bonds to Quasi-liquids. JACS Au. 2022;2(3):543–561.
[58] Su Y-Z, Fu Y-C, Wei Y-M, et al. The electrode/ionic liquid interface: electric double layer and metal electrodeposition. Chemphyschem. 2010;11(13):2764–2778.
[59] Wang X, Salari M, Jiang D, et al. Electrode material–ionic liquid coupling for electrochemical energy storage. Nat Rev Mater. 2020;5(11):787–808.
[60] Santos AFM, Cruz C, Godinho MH, et al. Synthesis and characterisation of ionic liquid crystals based on substituted pyridinium cations. Liq Cryst. 2022;49(13):1809–1821.
[61] Santos AFM, Figueirinhas JL, Dias CJ, et al. Study of the mesomorphic properties and conductivity of *n*-alkyl-2-picolinium ionic liquid crystals. J Mol Liq. 2023;377: 121456.
[62] Arkas M, Paleos CM, Skoulios A. Crystal and liquid crystal behaviour of *N*-cyanoalkyl-*N*-alkyl-*N*, *N*-dimethylammonium bromides: role of the dipole interactions of the cyano groups. Liq Cryst. 1997;22(6): 735–742.
[63] Ji Y, Shi R, Wang Y, et al. Effect of the chain length on the structure of ionic liquids: from spatial heterogeneity to ionic liquid crystals. J Phys Chem B. 2013;117(4): 1104–1109.
[64] Sharma VS, Vekariya RH, Sharma AS, et al. Mesomorphic properties of liquid crystalline compounds with chalconyl central linkage in two phenyl rings. Liq Cryst Today. 2017;26(3):46–54.
[65] Kremer F, Różański SA. The dielectric properties of semiconducting disordered materials. In: Kremer F, and Schönhals A, editors. Broadband dielectric spectroscopy. Berlin, Germany: Springer; 2003. pp. 475–494.
[66] Sangoro JR, Iacob C, Serghei A, et al. Universal scaling of charge transport in glass-forming ionic liquids. Phys Chem Chem Phys. 2009;11(6):913–916.
[67] Mao X. Rational design of charge-functional materials: insights from molecular engineering and operando imaging. MRS Bull. 2021;46(3):273–279.
[68] Volgmann K, Epp V, Langer J, et al. Solid-state nmr to study translational Li ion dynamics in solids with low-dimensional diffusion pathways. Zeitschrift für Phys Chemie. 2017;231:1215–1241.